J. Korean Inst. Electr. Electron. Mater. Eng.
Vol. 36, No. 5, pp. 505-512 September 2023
doi: https://doi.org/10.4313/JKEM.2023.36.5.11
ISSN 1226-7945(Print), 2288-3258(Online)

Early Stage Report : Graduate Research

Effects of High-Energy Ball Milling and Sintering Time on the Electric-Field-Induced Strain Properties of Lead-Free BNT-Based Ceramic Composites

Nga-Linh Vu[1], Trang An Duong[1], Dae-Jun Heo[1,2], Thi Hinh Dinh[3], Chang Won Ahn[4], Byeong Woo Kim[5], Hyoung-Su Han[1], and Jae-Shin Lee[1]

[1] School of Materials Science and Engineering, University of Ulsan, Ulsan 44610, Korea

[2] Materials Analysis Laboratory, DEA-IL Corporation, Ulsan 44914, Korea

[3] Faculty of Materials Science and Engineering, Phenikaa University, Hanoi 12116, Viet Nam

[4] Department of Physics and EHSRC, University of Ulsan, Ulsan 44610, Korea

[5] Department of Electrical Engineering, University of Ulsan, Ulsan 44610, Korea

(Received July 10, 2023; Revised August 4, 2023; Accepted August 9, 2023)

Abstract: This study investigated crystal structures, microstructures, and electric-field-induced strain (EFIS) properties of Bi-based lead-free ferroelectric/relaxor composites. $Bi_{1/2}(Na_{0.82}K_{0.18})_{1/2}TiO_3$ (BNKT) as a ferroelectric material and $0.78Bi_{1/2}(Na_{0.78}K_{0.22})_{1/2}TiO_3$-$0.02LaFeO_3$ (BNKT2LF) as a relaxor material were synthesized using a conventional solid-state reaction method, and the resulting BNKT2LF powders were subjected to high-energy ball milling (HEBM) after calcination. As a result, HEBM proved a larger average grain size of sintered samples compared to conventional ball milling (CBM). In addition, the increased sintering time led to grain growth. Furthermore, HEBM treatment and sintering time demonstrated a significant effect on EFIS of BNKT/BNKT2LF composites. At 6 kV/mm, 0.35% of the maximum strain (S_{max}) was observed in the HEBM sample sintered for 12 h. The unipolar strain curves of CBM samples were almost linear, indicating almost no phase transitions, while HEBM samples displayed phase transitions at 5~6 kV/mm for all sintering time levels, showing the highest S_{max}/E_{max} value of 700 pm/V. These results indicated that HEBM treatment with a long sintering time might significantly enhance the electromechanical strain properties of BNT-based ceramics.

Keywords: Lead-free piezoelectric ceramics, Relaxor, Incipient piezoelectrics, High energy ball milling

Piezoelectric ceramics have become increasingly important in micro-controllable sensor and actuator applications, as they can convert mechanical energy into electrical energy and vice versa. One of the most widely used materials in piezoelectric ceramics is lead zirconate titanate (PZT), which has been employed since the 1950s [1]. However, concerns over the health and environmental impacts of the harmful lead content in PZT have driven the search for lead-free materials as a promising alternative that has been very interested in the last 20 years [1-3]. Unfortunately, replacing lead-based materials with lead-free alternatives is still challenging because lead-free alternatives exhibited comparatively poor piezoelectric properties [3,4]. This limitation has arisen from lower

✉ **Hyoung-Su Han; hsejs@ulsan.ac.kr**

electromechanical coupling coefficients, phase transitions, and restricted material choices. However, ongoing efforts in material composition adjustments, structural modifications, and advanced processing techniques have been offering promising prospects for enhancing the performance of lead-free piezoelectric materials in the future.

In recent years, (Bi, Na)TiO_3 (BNT)-based solid solutions have emerged as highly promising lead-free ceramics due to their abnormally large electromechanical strain properties [5-7]. In the study conducted by Zhang et al. [5], a giant EFIS was reported in BNT–BT–KNN system, reaching a normalized strain Smax/Emax of 560 pm/V. It was clarified that the abnormally large electromechanical strain in BNT-based ceramics originated from the electric-field-induced phase transition from ergodic relaxor (ER) to ferroelectric (FE) as incipient piezoelectrics [6-8]. However, achieving large strain in BNT-based ceramics often requires a high electric field (generally, 6~8 kV/mm). Hence, this work focused on conducting research studies to investigate strategies aimed at reducing the electric field magnitude and achieving a significant increase in strain.

Two commonly employed approaches for enhancing the electrical properties of lead-free ceramics are through the utilization of advanced synthesis methods and the incorporation of treatments during the synthesis process. A promising advanced synthesis method has been proposed for achieving significant electric-field-induced-strain (EFIS) at low-driving fields is the use of ferroelectric/relaxor (FE-RE) ceramic composites. For incipient piezoceramics, a composite method consisting of a relaxor (matrix) and a ferroelectric phase (seed) has been shown to be effective in inducing a phase transformation to obtain a giant strain at the low electric field [5,9-12]. Dinh et al. [10] reported that a maximum S_{max}/E_{max} of 761 pm/V at 4 kV/mm when 30 wt.% ferroelectric BNKT seed material was added in the relaxor BNKLTT matrix, which was higher than that of the single ferroelectric or relaxor phase. Strain of 0.27% and 0.29%, for 0.94BNKT-0.06BA with 10% BNT and 0.93BNKT-0.07BA with 20% BNT at 4 kV/mm, are given in the report of Lee et al. [11].

As a second promising approach, treatments have been utilized to enhance the electrical properties of lead-free ceramics. Traditionally, ceramic powders prepared using conventional ball milling (CBM) as a solid-state reaction. However, a more recent treatment called high-energy ball milling (HEBM) has been explored as a promising technique to improve the sinterability and electromechanical strain properties of lead-free piezoelectric ceramics [13-17]. In the research of Han et al. [15], HEBM showed a reduction in particle size of $Bi_{1/2}(Na_{0.82}K_{0.18})_{1/2}TiO_3$/$0.78Bi_{1/2}(Na_{0.78}K_{0.22})_{1/2}TiO_3$-$0.02LaFeO_3$ (BNKT/BNKT2LF) ceramic composites in comparison to CBM, also the highest S_{max}/E_{max} of 600 pm/V at 4 kV/mm was obtained with a 30 min treated HEBM sample, which is comparable to a single BNKT2LF ceramics. Miclea et al. [16] reported that the average grain size of soft PZT powder prepared by CBM was in micro-size, while powder prepared by HEBM was in nano-size, and showed good piezoelectric characteristics: a planar coupling factor of 0.66, a displacement constant d_{33} of 550 pm/V, a mechanical quality factor of 85, and a relative dielectric constant of 3800. HEBM led to microstructures of PZT-based ceramics that were smaller-grained than CBM in the report of Lee et al. [17]. The planar piezoelectric coupling coefficient and piezoelectric constant of $Pb(Zr_{0.475}Ti_{0.525})$-O_3-$Pb(Mg_{1/3}Nb_{2/3})O_3$-$Pb(Fe_{1/2}Nb_{1/2})O_3$ (PFMNZT) ceramics sintered at 850°C for 2 h were 0.64 and 511 pC/N, respectively [17]. The explanation for the above results could be that HEBM has a higher mechanical stress level than CBM which leads to a decrease in the particle size and thus an increase in the sinterability of ceramics. In addition, the sintering time also played a crucial role in achieving high density and improving electrical properties of lead-free ceramic composites [18,19].

Therefore, this study investigated the effects of HEBM treatment on microstructures and electromechanical strain properties of BNKT/BNKT2LF composites with various sintering times (1, 2, 6, 12 h at 1,150°C and 0 h at 1,175°C). For preparing BNKT/BNKT2LF composites, $Bi_{1/2}(Na_{0.82}K_{0.18})_{1/2}TiO_3$ (BNKT) as FE phase and $0.78Bi_{1/2}(Na_{0.78}K_{0.22})_{1/2}TiO_3$-$0.02LaFeO_3$ (BNKT2LF) as RE matrix were selected in this work.

Ceramic powders conforming to the chemical formula $Bi_{1/2}(Na_{0.82}K_{0.18})_{1/2}TiO_3$ (BNKT) and $0.78Bi_{1/2}(Na_{0.78}K_{0.22})_{1/2}TiO_3$-$0.02LaFeO_3$ (BNKT2LF) were synthesized by using a conventional solid-state reaction route. Reagent grade Bi_2O_3, Na_2CO_3, K_2CO_3, La_2CO_3, Fe_2O_3, and TiO_2 (99.9%, High Purity Chemicals, Japan) powders were used as raw materials. These raw materials were first put in a drying oven at 100°C for 24 h to remove moisture and then weighed according to the stoichiometric formula as BNKT and BNKT2LF,

respectively. The powders were ball-milled in ethanol with zirconia balls for 24 h, dried at 80℃ for 24 h, and calcined at 850℃ for 2 h in a covered alumina crucible. After calcination, BNKT2LF powders as relaxor (RE) materials were high energy ball-milled (Planetary Mills, Fritsch GmbH, Germany) in ethanol with steel balls for 30 minutes. After that BNKT powders as 10 wt% ratio was mixed in conventional ball milling (CBM)-/or were high energy ball milling (HEBM)-derived BNKT2LF powders with polyvinyl alcohol (PVA) as a binder and then pressed into green discs with a diameter of 12 mm under a uniaxial pressure of 98 MPa. These green pellets were sintered in a covered alumina crucible at 1,175℃ for 0 h and at 1,150℃ for 1, 2, 6, and 12 h in air, respectively. The thermally etched surface micrographs of samples were imaged by using field-emission scanning electron microscopy (FE-SEM, JEOL JSM-65OFF, USA), and density of sintered samples was measured by the Archimedes method. The crystal structure was characterized by X-ray diffractometer (XRD, RAD III, Rigaku, Japan). For electrical measurements, a silver paste was screen printed on both sides of specimens and subsequently burnt at 700℃ for 30 min. The ferroelectric hysteresis loops and electric-field-induced strain was measured in a silicon oil bath using a modified Sawyer-Tower circuit and a linear variable differential transducer (LVDT), respectively.

Figures 1(a) and (b) illustrate the morphology of BNKT2LF ceramic powders, which was obtained via conventional ball milling (CBM) and high-energy ball milling (HEBM), respectively. CBM-derived powders as Fig. 1(a) displayed spherical particles with size of range from 0.5 to 1 μm. Conversely, HEBM-derived powders in Fig. 1(b) were indicated as a bimodal distribution that consisted of the spherical-shaped and nano-size of the irregular-shaped particles [as indicated in Fig. 1(b) with yellow arrow]. It is evident that the HEBM treatment can significantly reduce particle size and might result in a heterogeneous distribution of particle size in comparison to the CBM-derived powders. Similar findings were reported [15-17]. The sintering behaviors of CBM- and HEBM-derived BNKT/BNKT2LF composites with various sintering time are presented in Fig. 1(c). As the sintering time increased, the linear shrinkage of the composites was significantly raised. Comparing the sintering times of 0 h, 1 h, and 2 h, the HEBM-derived composites exhibited slightly higher shrinkage compared to the CBM-derived composites. However, when sintering time was extended to 6 h and 12 h, higher shrinkage values were

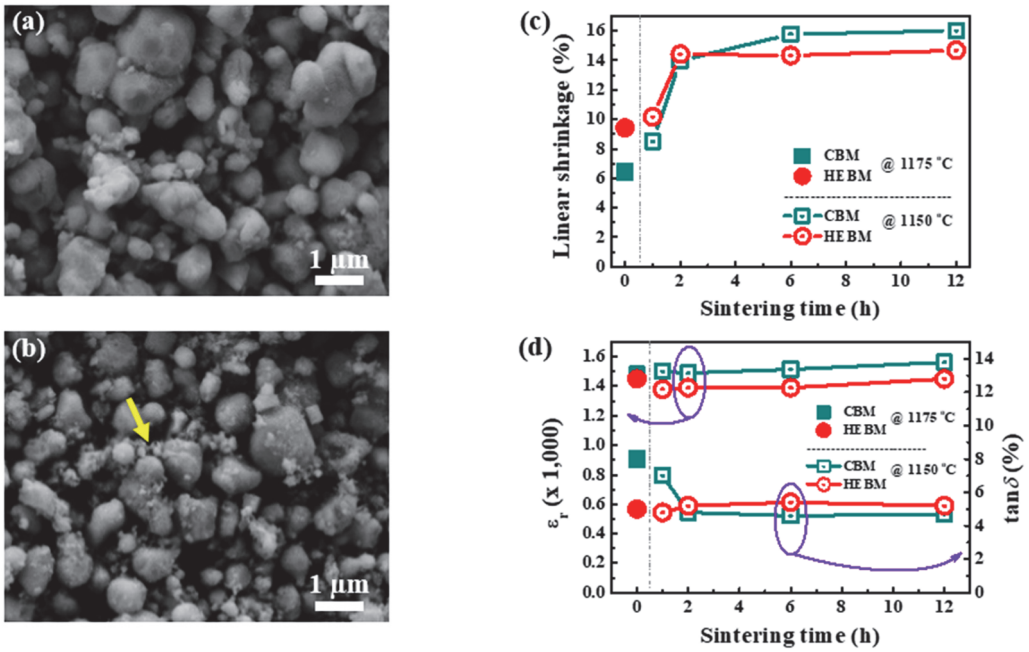

Fig. 1. Morphology of (a) CBM-derived and (b) HEBM-derived BNKT2LF ceramic powders; (c) sinterability, and (d) dielectric properties of BNKT/BNKT2LF composites as a function of sintering time.

observed at the CBM-derived composites. HEBM-derived composites experienced a rapid shrinkage of 14% within a 2 h, which then remained relatively stable during extended sintering time. In contrast, CBM-derived composites exhibited a shrinkage of 16% and underwent minimal changes after 6 h of sintering. This observation highlighted the significant impact of nano-sized particles in HEBM-derived powders has been shown to influence sintering behavior to quickly achieve a saturation of shrinkage. Consequently, the implementation of HEBM treatment allowed for a reduction in the optimal sintering temperature from 1,175℃ to 1,150℃ while a satisfactory sinterability was still ensuring. Similar results were observed by Kong et al. [13,20] in HEBM-treated PZT ceramics and Micelea et al. [16]. Figure 1(d) demonstrates dielectric properties of BNKT/BNKT2LF composites as a function of sintering time. At all sintering times, the dielectric constants of CBM-derived composites were slightly higher than that of HEBM-derived composites. The dielectric loss of HEBM-derived composites remained approximately constant at over 5.5% for all sintering times. In contrast, CBM-derived composites exhibited a significant change in dielectric loss. Initially, when sintering time was 0 h, dielectric loss of CBM-derived composites was approximately one and a half times higher than that of HEBM-derived composites, exceeding 8%. However, as sintering time increased to 1 h and then 2 h, dielectric loss of CBM-derived composites showed a rapid decrease. At this point, dielectric loss values of the CBM-derived composites became slightly smaller than those of HEBM-derived composites, measuring less than 5.5%. Subsequently, these values remained nearly unchanged when sintering time was increased to 6 h and 12 h.

Figure 2 presents microstructures of the polished and thermally-etched surfaces for CBM (top)- and HEBM (bottom)-derived BNKT/BNKT2LF composites with respect to sintering time. As sintering time increased, both CBM- and HEBM-derived composites demonstrated the enhanced densification and an increase in average grain size with decreasing the number of visible pores. These observations were further supported by Fig. 3(a). Additionally, it is noted that average grain size of the HEBM-derived samples was

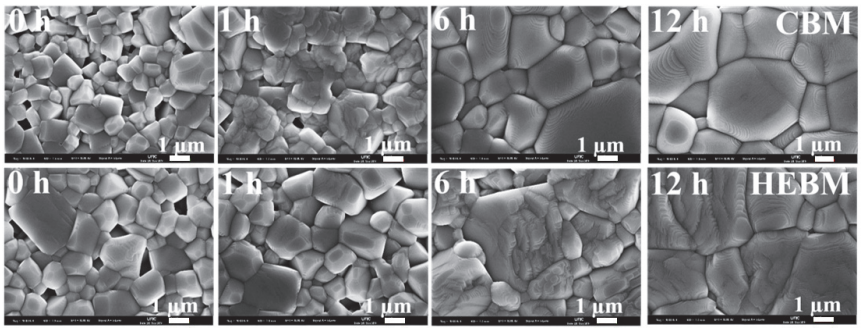

Fig. 2. Thermally-etched surface morphologies of CBM (top)- and HEBM (bottom)-derived BNKT/BNKT2LF composites as a function of sintering time.

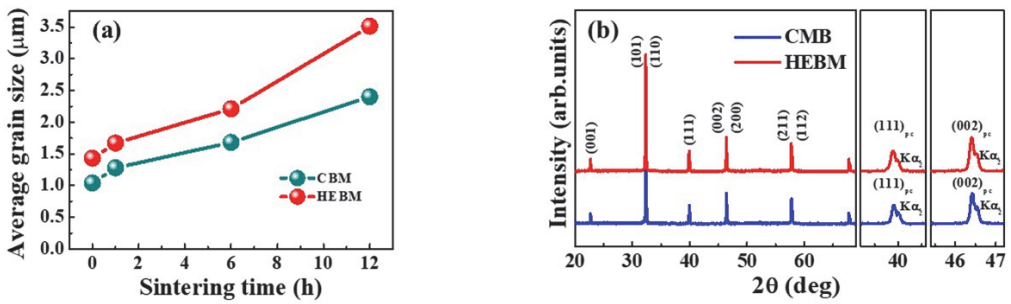

Fig. 3. (a) Average grain size as a function of sintering time and (b) X-ray diffraction patterns of CBM- and HEBM-derived BNKT/BNKT2LF composites (samples were sintered at 1,150℃ for 2 h).

larger in comparison with the CBM-derived samples. It is suggested that this different average grain size between HEBM- and CBM-derived samples is originated from the existence of nano-sized particles (the mechanically crashed poeders) in HEBM-derived powders [21].

Figure 3(b) displays X-ray diffraction patterns of CBM- and HEBM-derived BNKT/BNKT2LF composites. It is revealed that the dominant structure in all samples was the perovskite structure, with no presence of secondary phases. The sharp and narrow peak profiles indicated a well-developed crystalline structure. According to the detailed diffraction patterns corresponding to (111) and (002), there was no significant peak splitting except for the presence of Kα2. This result was consistently observed in the sintered samples with different time. These observed features were also documented in BNT ceramics [22-24].

Figure 4(a) displays bipolar strain (*S*-*E*) curves of CBM- and HEBM-derived BNKT/BNKT2LF composites, highlighting influence of sintering time and applied electric fields. Figure 4(b) presents the extracted parameters as the maximum strain (S_{max}) and negative strain (S_{neg}) from Fig. 4(a). Bipolar strain curves for HEBM-derived composites exhibited a feature of the large strain curve with neglectable S_{neg} regardless of sintering time, while those of CBM-derived composites were significantly changed by sintering time. In the case of bipolar strain for 1 h sintered CBM-derived composites, low strain performances in all the applied electric fields were revealed. It can assume that poor sinterability (in Fig. 1) for 1 h sintered CBM-derived composites was responsible for low strain performances. As the sintering time increased to 6 h or 12 h, strain of CBM-derived composites was drastically increased with significantly expending S_{neg} except for 3 kV/mm as an applied electric field. These results imply that an electric field of at least 4 kV/mm was required for large strain based on the electric-field-induced phase transition in 6 h or 12 h sintered CBM-derived composites. On the other hand, bipolar strain properties for 1 h sintered HEBM-derived composites were larger than that of CBM-derived composites, which steadily increased by the applied electric field. Upon increasing sintering time to 6 h, strain of HEBM-derived composites

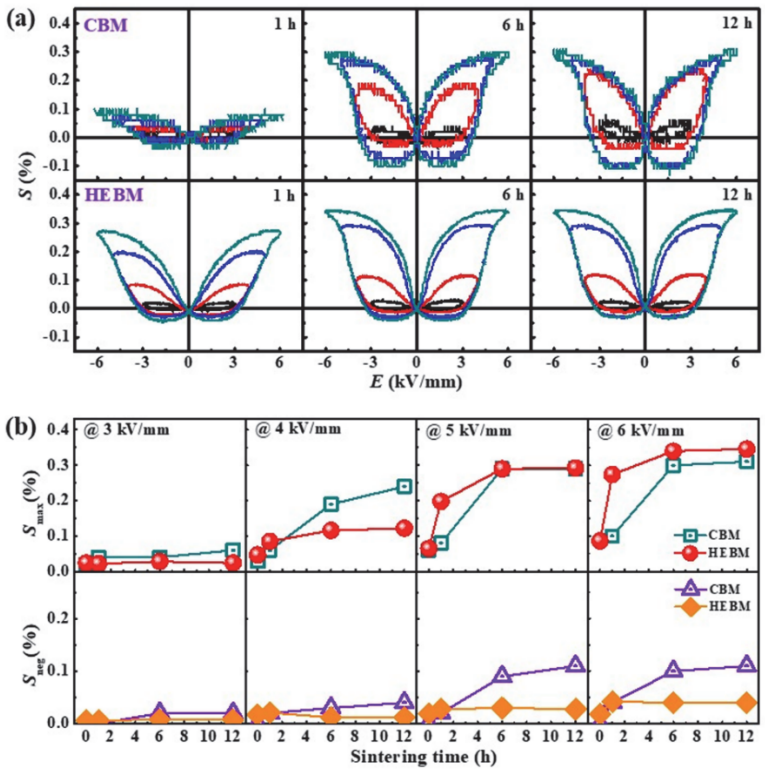

Fig. 4. (a) Bipolar strain curves as a function of sintering time and (b) the extracted parameters as maximum strain (S_{max}) and negative strain (S_{neg}) with different sintering time and applied electric fields of CBM- and HEBM-derived BNKT/BNKT2LF composites.

reached a highly stable state at all electric fields. This stability was maintained even when the sintering time was further increased to 12 h, as strain values remained nearly unchanged. Interestingly, the drastic increases in strain properties were obtained by applying electric fields of 5~6 kV/mm in 6 h and 12 h sintered HEBM-derived composites. It implies that an electric field of at least 4 kV/mm was needed to induce large strain in 6 h and 12 h sintered HEBM-derived composites. These changes in strain properties are compared in Fig. 4(b).

To clarify the differences in strain properties between CBM- and HEBM-derived BNKT/BNKT2LF composites, unipolar strain curves as a function of sintering time are illustrated in Fig. 5(a). Subsequently, S_{max}/E_{max} values (maximum strain to maximum electric field) were calculated with varying sintering times and applied electric fields, which were plotted in Fig. 5(b). For HEBM-derived composites, the features of large strain properties (with large hysteresis) were revealed and the drastic increases in strain properties were observed at 5~6 kV/mm for all sintering times [5-7]. As discussed in Fig. 4, it implies that HEBM-derived composites can be categorized as ergodic relaxor (ER) [6,7]. Furthermore, 5~6 kV/mm as an applied electric field is needed to induce phase transition from ER to ferroelectrics (FE) in HEBM-derived composites. In contrast, 1 h sintered CBM-derived composites exhibited nearly linear unipolar strain curves, indicating no phase transitions. With increasing sintering times of 6 h and 12 h, unipolar strain was drastically increased. Interestingly, the highest unipolar strain was obtained at 4 kV/mm. With increasing the applied electric field to 5 kV/mm or 6 kV/mm, unipolar strain was rapidly decreased with declining strain hysteresis. It can be assumed that the degradation of unipolar strain properties with increasing electric field is originated from the polarized ferroelectricity in CBM-derived composites. Besides, this assumption can be strongly supported by the observed S_{neg} in bipolar strain curves (in Fig. 4) of 6 h and 12 h sintered CBM-derived composites. Accordingly, at low electric fields of 3~4 kV/mm, S_{max}/E_{max} values of CBM-derived composites were higher than those of HEBM-derived composites. However, at high electric fields of 5~6 kV/mm, S_{max}/E_{max} values of HEBM-derived composites were higher than those of CBM-derived composites. HEBM-derived samples exhibited a maximum S_{max}/E_{max} value of approximately 700 pm/V, which was achieved at 5 kV/mm after 12 h of sintering time. On the other hand, CBM-derived samples attained a similar S_{max}/E_{max} value of approximately 700 pm/V at 4 kV/mm after 12 h of sintering time.

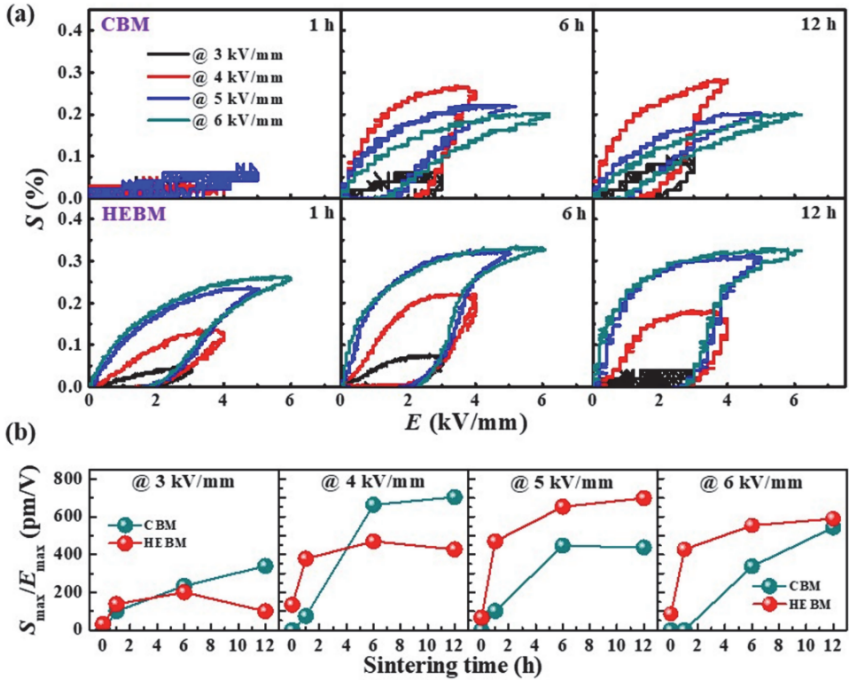

Fig. 5. (a) Unipolar strain curves as a function of sintering time and (b) S_{max}/E_{max} values with different sintering time and applied electric fields of CBM- and HEBM-derived BNKT/BNKT2LF composites.

Accordingly, we successfully demonstrated that the different strain behaviors between HEBM-derived samples and CBM-derived samples are originated from the different state of stabilized relaxor based on initial powders. For better understanding of the exact mechanism on these strain behaviors, it is suggested that the advanced analyses are needed further.

As conclusions, this study investigated the effects of HEBM treatment and sintering time on the strain properties of BNKT/BNKT2LF composites. HEBM treatment resulted in a larger average grain size compared to CBM. Moreover, increasing the sintering time promoted grain growth in BNKT/BNKT2LF composites. These findings indicated that combining HEBM treatment with a longer sintering time significantly enhances the strain properties of BNKT/BNKT2LF composites. Specifically, CBM-derived samples exhibited a large strain under low electric fields and long sintering times. On the other hand, the improved strain properties were observed in HEBM-derived samples under high electric fields. These results suggest that the combination of HEBM treatment and a long sintering time holds great potential for controlling electromechanical strain properties of lead-free BNT-based ceramics.

ORCID

Hyoung-Su Han https://orcid.org/0000-0002-7423-2862

ACKNOWLEDGEMENTS

This study was supported by the National Research Foundation (NRF) of the Republic of Korea (Grants 2020R1C1C1007375). CW Ahn acknowledges financial support from the Basic Science Research Program through the National Research Foundation (NRF) of the Republic of Korea (RS-2023-00245221).

REFERENCES

[1] C. H. Hong, H. P. Kim, B. Y. Choi, H. S. Han, J. S. Son, C. W. Ahn, and W. Jo, *J. Materiomics*, **2**, 1 (2016). doi: https://doi.org/10.1016/j.jmat.2015.12.002

[2] J. Rödel, K. G. Webber, R. Dittmer, W. Jo, M. Kimura, and D. Damjanovic, *J. Eur. Ceram. Soc.*, **35**, 1659 (2015). doi: https://doi.org/10.1016/j.jeurceramsoc.2014.12.013

[3] W. S. Kang, C. H. Hong, Y. J. Lee, G. Choi, D. J. Shin, D. H. Lim, S. J. Jeong, and W. Jo, *J. Korean Ceram. Soc.*, **56**, 549 (2019). doi: https://doi.org/10.4191/kcers.2019.56.6.03

[4] J. Rödel, W. Jo, K.T.P. Seifert, E. M. Anton, T. Granzow, and D. Damjanovic, *J. Am. Ceram. Soc.*, **92**, 1153 (2009). doi: https://doi.org/10.1111/j.1551-2916.2009.03061.x

[5] S. T. Zhang, A. B. Kounga, E. Aulbach, H. Ehrenberg, and J. Rödel, *Appl. Phys. Lett.*, **91**, 112906 (2007). doi: https://doi.org/10.1063/1.2783200

[6] W. Jo, R. Dittmer, M. Acosta, J. Zang, C. Groh, E. Sapper, K. Wang, and J. Rödel, *J. Electroceram.*, **29**, 71 (2012). doi: https://doi.org/10.1007/s10832-012-9742-3

[7] H. S. Han, W. Jo, J. K. Kang, C. W. Ahn, I. Won Kim, K. K. Ahn, and J. S. Lee, *J. Appl. Phys.*, **113**, 154102 (2013). doi: https://doi.org/10.1063/1.4801893

[8] H. Zhang, C. Groh, Q. Zhang, W. Jo, K. G. Webber, and J. Rödel, *Adv. Electron. Mater.*, **1**, 1500018 (2015). doi: https://doi.org/10.1002/aelm.201500018

[9] C. Groh, D. J. Franzbach, W. Jo, K. G. Webber, J. Kling, L. A. Schmitt, H. J. Kleebe, S. J. Jeong, J. S. Lee, and J. Rödel, *Adv. Funct. Mater.*, **24**, 356 (2014). doi: https://doi.org/10.1002/adfm.201302102

[10] T. H. Dinh, C. H. Yoon, J. K. Kang, Y. H. Hong, and J. S. Lee, *Ferroelectrics*, **487**, 142 (2015). doi: https://doi.org/10.1080/00150193.2015.1071619

[11] D. S. Lee, D. H. Lim, M. S. Kim, K. H. Kim, and S. J. Jeong, *Appl. Phys. Lett.*, **99**, 062906 (2011). doi: https://doi.org/10.1063/1.3621878

[12] D. S. Lee, S. J. Jeong, M. S. Kim, and J. H. Koh, *J. Appl. Phys.*, **112**, 124109 (2012). doi: https://doi.org/10.1063/1.4770372

[13] L. B. Kong, J. Ma, W. Zhu, and O. K. Tan, *J. Alloys Compd.*, **322**, 290 (2001). doi: https://doi.org/10.1016/S0925-8388(01)01256-7

[14] L. B. Kong, J. Ma, H. Huang, and R. F. Zhang, *J. Alloys Compd.*, **345**, 238 (2002). doi: https://doi.org/10.1016/S0925-8388(02)00400-0

[15] H. S. Han, D. J. Heo, T. H. Dinh, C. H. Lee, J. K. Kang, C. W. Ahn, V.D.N. Tran, and J. S. Lee, *Ceram. Int.*, **43**, 7516 (2017). doi: https://doi.org/10.1016/j.ceramint.2017.03.038

[16] C. Miclea, C. Tanasoiu, A. Gheorghiu, C. F. Miclea, and V. Tanasoiu, *J. Mater. Sci.*, **39**, 5431 (2004). doi: https://doi.org/10.1023/B:JMSC.0000039260.82430.f9

[17] J. S. Lee, M. S. Choi, N. V. Hung, Y. S. Kim, I. W. Kim, E. C. Park, S. J. Jeong, and J. S. Song, *Ceram. Int.*, **33**, 1283 (2007). doi: https://doi.org/10.1016/j.ceramint.2006.04.017

[18] K. Orlik, Y. Lorgouilloux, P. Marchet, A. Thuault, F. Jean, M. Rguiti, and C. Courtois, *J. Eur. Ceram. Soc.*, **40**, 1212 (2020).

doi: https://doi.org/10.1016/j.jeurceramsoc.2019.12.010

[19] S. K. Gupta, B. J. Gibbons, P. Mardilovich, and D. P. Cann, *J. Appl. Phys.*, **130**, 184102 (2021).
doi: https://doi.org/10.1063/5.0067319

[20] L. B. Kong, J. Ma, H. T. Huang, W. Zhu, and O. K. Tan, *Mater. Lett.*, **50**, 129 (2001).
doi: https://doi.org/10.1016/S0167-577X(00)00429-8

[21] L. Cheng, P. Liu, S. X. Qu, and H. W. Zhang, *J. Alloys Compd.*, **581**, 553 (2013).
doi: https://doi.org/10.1016/j.jallcom.2013.06.133

[22] H. S. Han, I. K. Hong, Y. M. Kong, J. S. Lee, and W. Jo, *J. Korean Ceram. Soc.*, **53**, 145 (2016).
doi: https://doi.org/10.4191/kcers.2016.53.2.145

[23] T. H. Dinh, J. K. Kang, J. S. Lee, N. H. Khansur, J. Daniels, H. Y. Lee, F. Z. Yao, K. Wang, J. F. Li, H. S. Han, and W. Jo, *J. Eur. Ceram. Soc.*, **36**, 3401 (2016).
doi: https://doi.org/10.1016/j.jeurceramsoc.2016.05.044

[24] T. H. Dinh, M. R. Bafandeh, J. K. Kang, C. H. Hong, W. Jo, and J. S. Lee, *Ceram. Int.*, **41**, S458 (2015).
doi: https://doi.org/10.1016/j.ceramint.2015.03.150